Supplementary Material (ESI) for Energy & Environmental Science


*Copper sulfide as a light absorber in wet-chemical synthesized Extremely Thin Absorber (ETA) solar cells*

Miles Page, Olivia Niitsoo, Yafit Itzhaik, David Cahen and Gary Hodes

# Supporting Information

## (1) Experimental

Glass coated with Fluorine-doped tin oxide was purchased from Hartford Glass Inc., and cut to 2.5 x 1 cm pieces. These were cleaned by sonicating in detergent solution and then ethanol, and dried in a $N_2$ stream. A dense $TiO_2$ layer was formed from titanium isopropoxide (Sigma-Aldrich) sol stabilized with diethanolamine, as described in [Y. Ohya, H. Saiki, T. Tanaka, Y. Takahashi, *J. Am. Ceram. Soc.*, 1996, **79**, 825]. This sol was spin-coated at 4000 rpm onto the FTO surface, annealed at 200 °C for 10 mins then at 500 °C for 30 mins. Five layers were applied following this procedure, resulting in a layer of 120 nm average thickness as determined in cross-section SEM.

1.0g of $TiO_2$ nanoparticles (P25, Degussa) were dispersed in 5 mL of ethanol. To this dispersion was added 1 mL of a 0.02 g/mL solution of poly(ethylene glycol) (MW 8000, Fluka) in acetonitrile. This dispersion was spin-coated onto the substrates at 3000 rpm, resulting in a layer of approx. 2 microns thickness by cross-section SEM. The electrodes were then annealed at 500 °C for 30 mins.

CdS layers were formed by CBD using the recipe described in [O. Niitsoo, S. Sarkar, C. Pejoux, S. Rühle, D. Cahen, G. Hodes, *J. Photochem. and Photobiol. A: Chemistry*, 2006, **181**, 306]. Deposition was carried out at 25 °C, typically for 15 mins. The electrodes were then removed, washed with water and then 0.1M $Na_2S$ (to convert any $Cd(OH)_2$ into CdS) and again with water, then dried in a $N_2$ stream.

In-OH-S buffer layers were formed also by CBD. The recipe described in [R. Bayon, C. Guillen, M. A. Martinez, *et al*., *J. Electrochem. Soc.*, 1998, **145**, 2775-2779] was modified to maximize the surface coverage for our system. We used a solution of $In_2(SO_4)_3$ (0.009 M) or $InCl_3$ (0.018 M) with thioacetamide (0.1 M), placed with the substrates in a water bath at $69^0$C, typically for 45m. The pH of this solution was 2.5-3. Unlike in the reference above, we did not acidify the solution any further, as we found that addition of acetic acid resulted in a more porous film with noticeable pinholes.

$Cu_{2-x}S$ was formed by topotactic exchange with CdS, using a bath of 10mM CuI in 1M KI. Exchange was typically carried out at 90 °C for 20 seconds. This process was carried out either on $TiO_2$ | CdS, $TiO_2$ | In-OH-S | CdS, or $TiO_2$ | In-OH-S | ZnS.

Before adding CuSCN, cells were soaked for 5 mins in aqueous LiSCN (0.5M), and the excess wiped off gently with tissue paper. They were then dried on a hot (80 °C) surface.

A saturated solution of CuSCN in dipropyl sulfide was prepared several days in advance. This was diluted by a factor of two to form the CuSCN deposition solution. Deposition was then carried out as described in [B. O'Regan, F. Lenzmann, *J. Phys. Chem. B*, 2004, **108**, 4342], using a syringe needle, sealed at the end and with 4 x 0.3mm holes drilled in the side of the needle. The electrode was held at a temperature of 75-80 °C during deposition. Higher temperatures result in the formation of large deposits of CuSCN on the top (as opposed to the internal) surface of the electrode, resulting in a loss of performance. Lower temperatures result in the growing CuSCN causing partial disintegration of the $TiO_2$ phase, resulting in loss of bicontinuity. However, the ideal temperature and concentrations are interdependent variables which are likely to require optimization for each individual deposition setup. In this configuration, with these cell sizes, typically ~0.5 mL of the deposition solution sufficiently fills the pores and leaves a layer of CuSCN, of the order 1 micron thickness, on the top surface of the electrode, preventing contact between the $TiO_2$ and the gold back contacts.

Gold contacts were deposited by electron beam evaporation, with a thickness of 50-100 nm. I-V measurements were made using a Keithley 230 programmable voltage source and a Keithley 2000 multimeter. The sample was illuminated by a tungsten-halogen lamp with operating voltage and distance set to give the same short circuit current as for the same cell under actual solar conditions (adjusted to 1000 $W/m^2$ by measuring the sunlight with an Eppley pyranometer). This calibration of the indoor lamp is different for CdS and Cu-S absorbers. Spectral response was measured with a commercial setup from Oriel Instruments, using a 550 W tungsten halogen lamp coupled to a monochromator for illumination. Bias from the lamp intensity spectrum was removed by calibrating the data against a silicon photodiode with known quantum efficiency vs. wavelength. This also allowed calculation of sample external quantum efficiencies.

Scanning Electron Micrographs were obtained using a Leo Ultra 55 microscope at 2 kV accelerating voltage.

TEM characterisation was performed on a Philips CM120 instrument, with samples placed on polymer-coated nickel grids.

(2) TEM characterization of the samples

S.I. Figure 1a shows an image of typical particles in the uncoated, porous $TiO_2$ film. A lattice spacing of 3.52 Å can be determined, corresponding to anatase [101]. The In-OH-S layer forms an amorphous, web-like coating over domains of $TiO_2$ particles (S.I. Figure 1b). No diffraction peaks can be observed either in image fourier transforms or by electron diffraction. CdS deposition then occurs primarily on this weblike layer (S.I. Figure 1c). The CdS is crystalline, with an observed lattice spacing of 3.36 Å, corresponding either to cubic CdS [111], or hexagonal [0002]. Finally the exchange to $Cu_{2-x}S$ results in no apparent morphological change to these particles (S.I. Figure 1d). However, electron diffraction shows a new lattice dimension of ~2.1Å, which corresponds to the primary diffraction peak of several $Cu_{2-x}S$ phases in the $0 < x < 0.2$ range. The closest match is to $Cu_{1.92}S$, hexagonal, [305]. We cannot, however, distinguish categorically between the many possible phases, and furthermore have not been able to find X-ray diffraction peaks, due probably to the small size of the crystals, in a matrix of larger $TiO_2$ particles. Analysis by energy-dispersive X-ray spectroscopy, taken with a sample on nickel grids and using a beryllium sample holder to avoid spurious detection of copper, shows that the sulfides are primarily $Cu_{2-x}S$, with much smaller amounts of Cd and In detected. (S.I. Table 1) Also, although the quantitative error in the EDS analysis is significant, and uncertain, it appears that there is more Cu than can be explained by the amount of S detected. This is probably the result of a certain amount of $Cu_2O$ (or CuO) formed during the air-anneal step.

| Element | Atom% |
|---|---|
| S | 27.9 |
| Cu | 61.3 |
| Cd | 5.3 |
| In | 5.6 |

**S.I. Table 1**. EDS Elemental analysis of particles from a TiO2 | In-OH-S | CdS-$Cu_{2-x}S$ electrode.

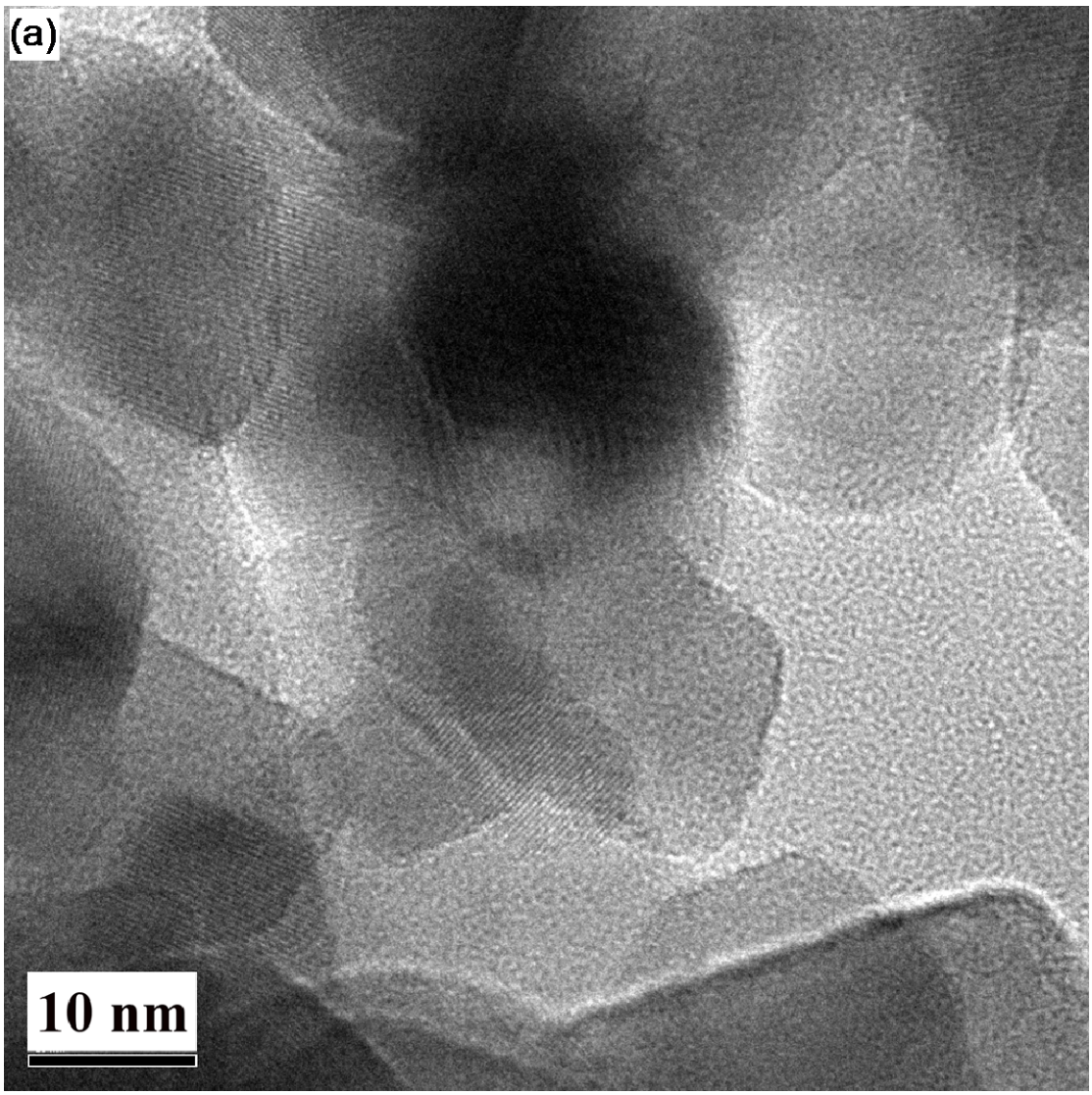


**S.I. Figure 1a**. *$TiO_2$ nanoparticle film before deposition of additional material.*

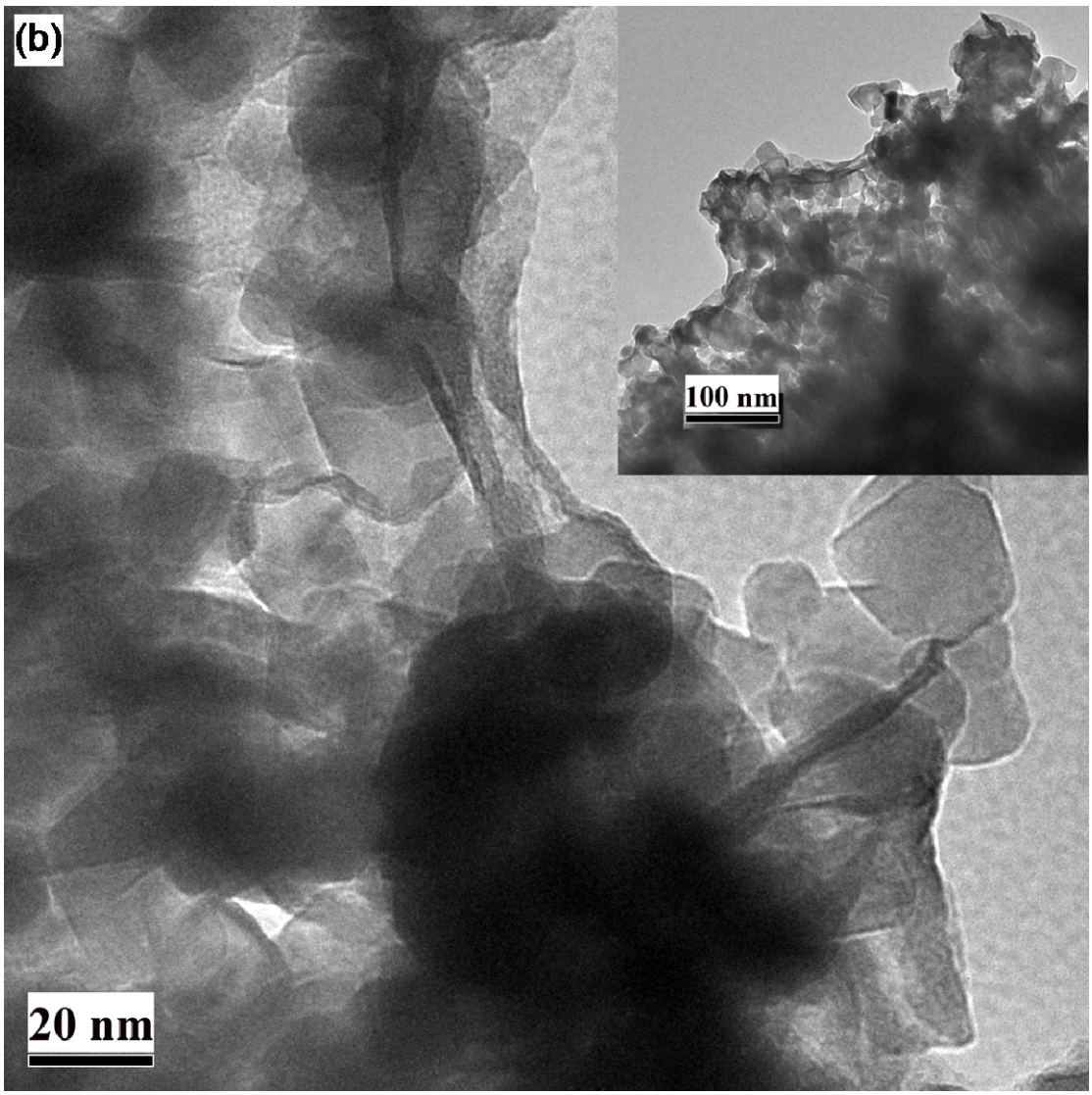


**S.I. Figure 1b**. *Amorphous In-OH-S coating on the $TiO_2$ nanoparticle film.*

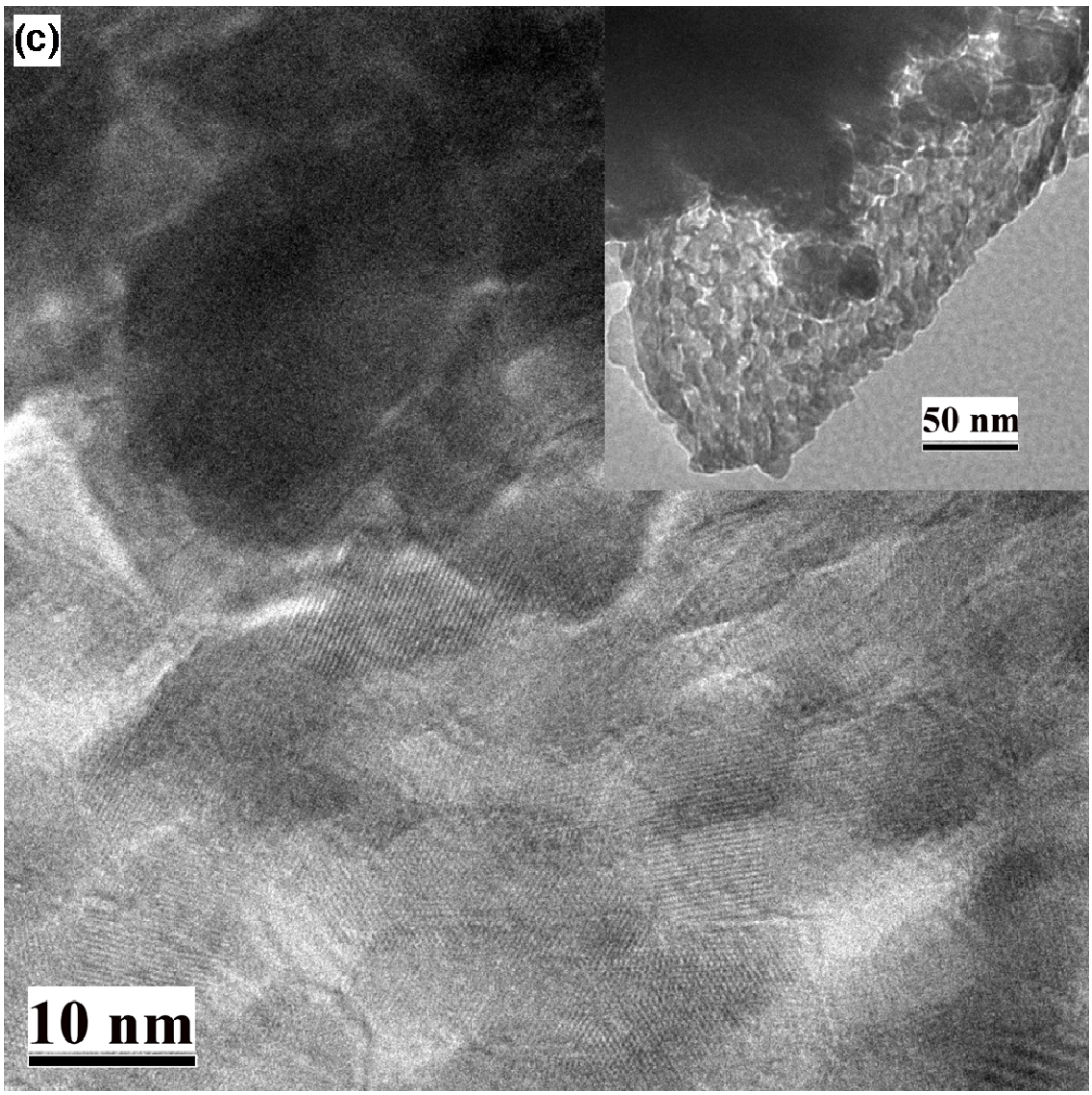


**S.I. Figure 1c**. *CdS nanocrystals on the $TiO_2$ | In-OH-S film.*

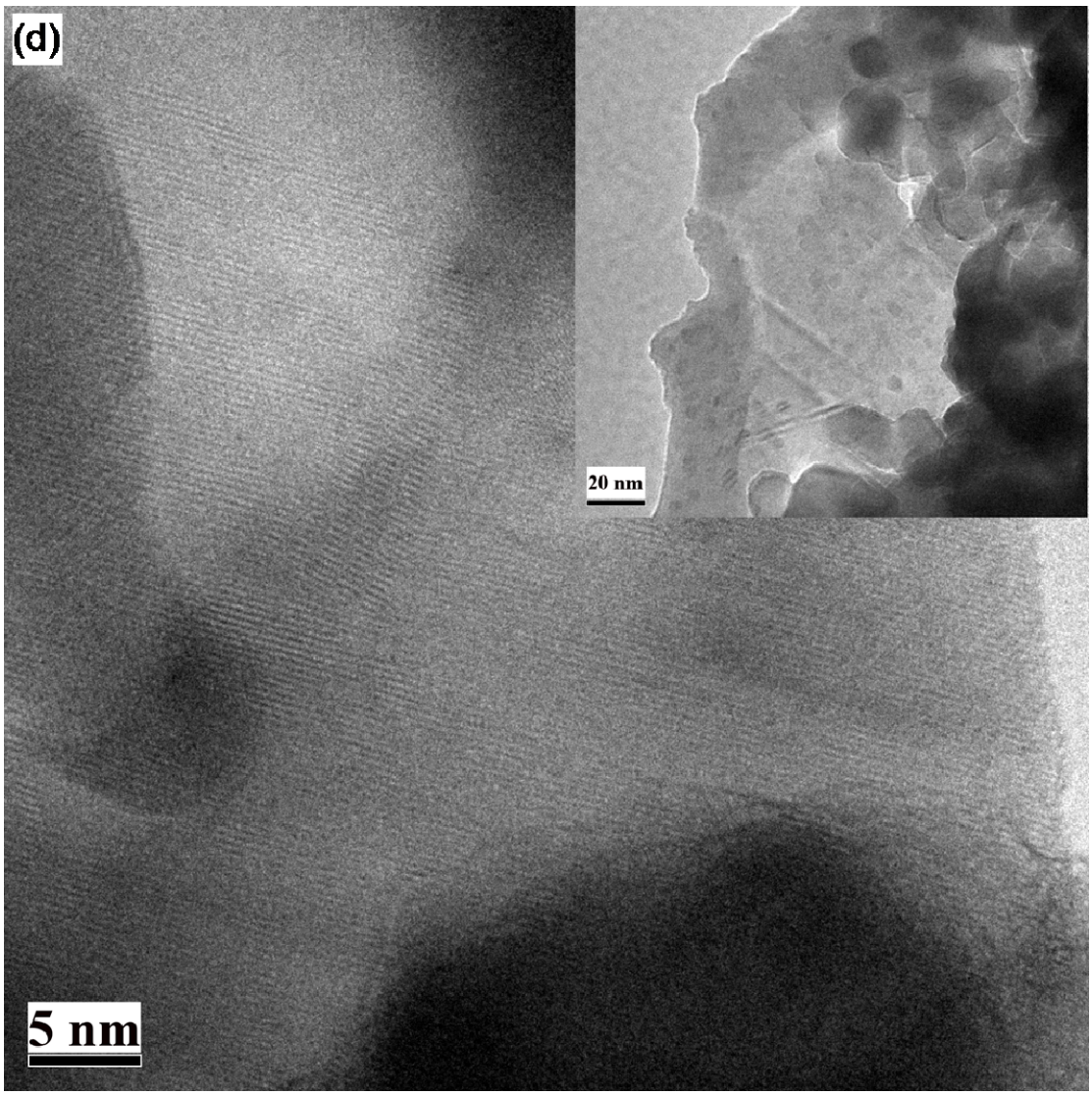


**S.I. Figure 1d**. *Close-up of $Cu_{2-x}S$, exchanged from CdS, on amorphous In-OH-S.*

## (3) Copper sulfide phases:

Determination of copper sulfide stoichiometry is possible using a chronopotentiometric titration described by Vedel *et al*. [E. Castel, J. Vedel, *Analusis*, 1975, **3**, 487] The potential of the $Cu_xS$ against a counter-electrode is measured as a function of time, under galvanostatic control. Performing this titration, we observe two end-points, one indicating formation of the chalcocite ($Cu_2S$) phase, and the second the reduction of $Cu_2S$ to Cu metal (which can be observed also by an accompanying colour change).
Figure 2 shows the UV-Vis spectra of the as-formed $Cu_{2-x}S$, and the same sample after titration to form $Cu_2S$.

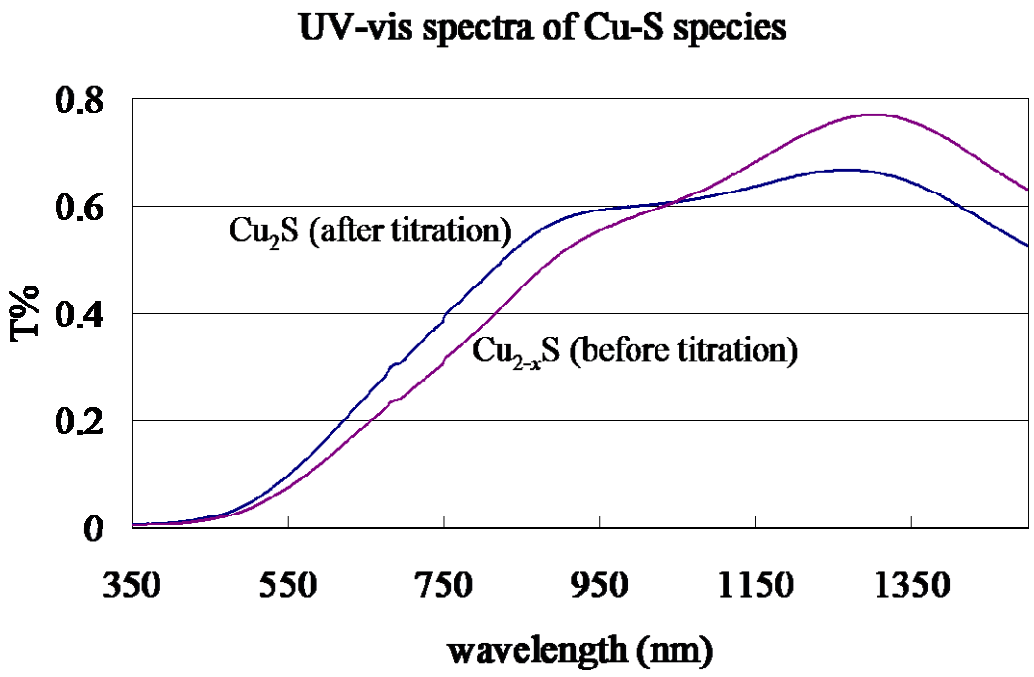


**S.I. Figure 2**: *UV-vis spectra of $Cu_{2-x}S$ formed from CdS deposited by CBD on FTO, before and after potentiometric titration to form $Cu_2S$.*

(4) Optical spectra of the various coating stages

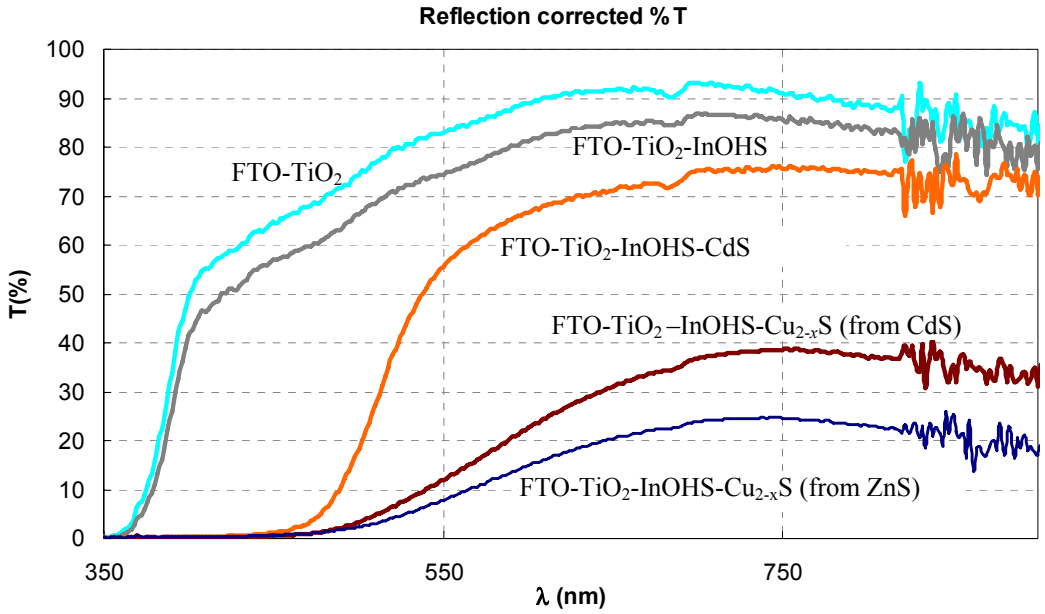


**S.I. Figure 3** *UV-vis spectra of cells in various stages of construction, from bare $TiO_2$, with added InOHS buffer layer, CdS, and finally with topotactically exchanged $Cu_{2-x}S$ from either CdS or ZnS.*

(5) Passivation of the $TiO_2$-CuSCN interface by adsorbed dodecylphosphonate.

Figure 4 shows the dark and light (tungsten halogen lamp) I-V curves of porous $TiO_2$/CuSCN junctions (including compact $TiO_2$ sublayer), with and without the alkylphosphonate monolayer. Inset is a zoomed version of the same curves. In the dark, the overall current passed as a function of voltage is lower with the monolayer than without, irrespective of the applied forward or reverse bias.

In the light, however, we see that in the forward direction, the rectification is poorer with the monolayer, than without it. This results in a larger current being passed in the positive direction at low voltages, despite the higher series resistance. This effect on the rectification is apparently the cause of the loss in voltage in the cells with the monolayer, relative to the plain interface, and is in accord with the increase in the work function of the $TiO_2$ film when the monolayer is applied (see article).

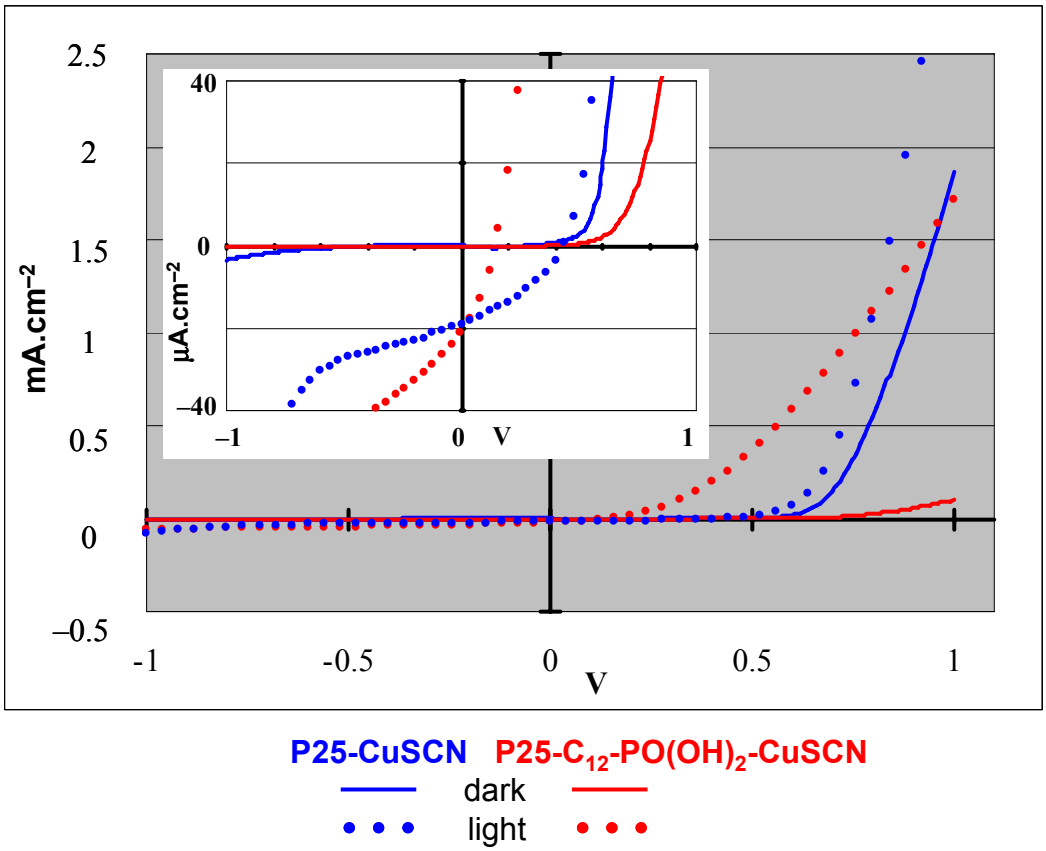


**S.I. Figure 4.** *Dark and light I-V curves of $TiO_2$ - CuSCN junction with and without an interfacial dodecylphosphonate monolayer.*